Rock Mechanics Study of Shaft Stability and Pillar Mining, Homestake Mine, Lead, SD

(In Three Parts)

3. Geomechanical Monitoring and Modeling Using UTAH3

By W. G. Pariseau, J. C. Johnson, M. M. McDonald, and M. E. Poad

UNITED STATES DEPARTMENT OF THE INTERIOR

UNITED STATES BUREAU OF MINES

U.S. Department of the Interior
Mission Statement

As the Nation's principal conservation agency, the Department of the Interior has responsibility for most of our nationally-owned public lands and natural resources. This includes fostering sound use of our land and water resources; protecting our fish, wildlife, and biological diversity; preserving the environmental and cultural values of our national parks and historical places; and providing for the enjoyment of life through outdoor recreation. The Department assesses our energy and mineral resources and works to ensure that their development is in the best interests of all our people by encouraging stewardship and citizen participation in their care. The Department also has a major responsibility for American Indian reservation communities and for people who live in island territories under U.S. administration.

Rock Mechanics Study of Shaft Stability and Pillar Mining, Homestake Mine, Lead, SD

(In Three Parts) #. Geomechanical Monitoring and Modeling Using UTAH3

By W. G. Pariseau, J. C. Johnson, M. M. McDonald, and M. E. Poad

CONTENTS

ILLUSTRATIONS

TABLES

UNIT OF MEASURE ABBREVIATIONS USED IN THIS REPORT

Metric Units

cm	centimeter	m	meter
h	hour	Mbyte	megabyte
kbyte	kilobyte	mm	millimeter
kg	kilogram	t	metric ton
kPa	kilopascal		

U.S. Customary Units

ft	foot	st	short ton
in	inch	tr oz	troy ounce

Rock Mechanics Study of Shaft Stability and Pillar Mining, Homestake Mine, Lead, SD

(In Three Parts)

3. Geomechanical Monitoring and Modeling Using UTAH3

By W. G. Pariseau,[1] J. C. Johnson,[2] M. M. McDonald,[3] and M. E. Poad[4]

ABSTRACT

A U.S. Bureau of Mines case study of pillar recovery in high-grade ore near the Ross shaft at the Homestake Mine, Lead, SD, has demonstrated the usefulness of the finite-element method for evaluating shaft pillar mining plans and shaft stability. In this study, borehole extensometers and other instruments were installed to provide data for model verification and to monitor shaft displacement. Results of a recalibrated two-dimensional model (UTAH2) confirmed the premining stability evaluation. However, after mining began, concern developed because of cracks and other signs of ground motion that appeared at considerable distances from the area of active pillar mining. An intense three-dimensional modeling effort using the computer modeling program UTAH3 was initiated. The results again showed the observed effects were within expectations and that the shaft would remain safe. Three-dimensional analyses of alternate pillar mining scenarios indicated that more of the shaft pillar ore reserve could be recovered than previously thought on the basis of two-dimensional analyses. This report focuses on startup and implementation of the three-dimensional model, calibration of the three-dimensional model, and application of the model to shaft pillar mining.

---

[1]McKinnon Professor of Mining Engineering, University of Utah, Salt Lake City, UT.
[2]Mining engineer, Spokane Research Center, U.S. Bureau of Mines, Spokane, WA.
[3]Research civil engineer, Spokane Research Center, retired.
[4]Supervisory mining engineer, Spokane Research Center.

INTRODUCTION

Because of the importance of shaft pillar design to the mining industry, research was undertaken at the Homestake Mine, Lead, SD, to investigate the extraction of valuable reserves within the Ross shaft pillar. The study was a cooperative effort and involved the U.S. Bureau of Mines (USBM), the Homestake Mining Co., and the University of Utah, Salt Lake City, UT. Table 1 shows the chronology of the main phases of the project.

Table 1.—Project chronology

Phase	Topic	Beginning date
1	2-dimensional premining analysis	April 1987.
2	Installation first instruments	October 1987.
3	Pillar mining begins	March 1988.
4	2-dimensional model validation	March 1989.
5	3-dimensional model 1	August 1990.
6	3-dimensional model 2	August 1991.
7	Additional instrumentation	July 1994.
8	3-dimensional model 3	March 1995.

The Homestake Mine is located in the northern Black Hills of South Dakota. Figure 1 shows the general layout of the mine, which is the oldest and deepest in North America. Development extends to the 8000 level (feet below the surface), with the Yates and Ross shafts providing access. About 8,398 kg (270,000 tr oz) of gold and 2,177 kg (50,000 tr oz) of silver are recovered from 1.5 million t (1.7 million st) of ore milled per year. Most of the ore reserve in the Ross shaft pillar lies between the 3200 and 3800 levels on the west side of the shaft. Stoping methods are mainly mechanized cut-and-fill and vertical crater retreat.

Pillar mining began below the 3650 level in late 1988. Shortly afterward, movement was observed on the 3200 level, where the shaft had been damaged in the early 1950's. In fact, it was the experience in the early 1950's that led to definition of the existing shaft pillar. Additional pillars within the shaft pillar were then defined in response to the threat of renewed ground movement.

The first RI of this series (Part 1. Premining Geomechanical Modeling Using UTAH2) described the general objectives of the study, site geology, practical shaft stability criteria, and the approach taken to the problem (Pariseau and others, 1995a). Discussed in detail were two-dimensional, finite-element simulations of (1) historical mining leading to the present shaft pillar and (2) future mining of the ore reserve in the shaft pillar. The results indicated that the Ross shaft remained in elastic ground, and thus, no large, catastrophic ground failures were likely. Hence, the pillar mining plan was considered safe.

In the second RI of the series (Part 2. Mine Measurements and Confirmation of Premining Results), instrument calibration and updating of the original two-dimensional, finite-element model were described (Pariseau and others, 1995b). This RI focused on a vertical section that allowed for sequential, lift-by-lift simulation of cut-and-fill extraction of the ore reserves in the shaft pillar and addressed several numerical modeling concerns that arose during the earlier premining study.

The approach to the particular problem of model calibration was (1) to install instruments prior to stoping for the purpose of measuring rock mass response to the first lifts taken in the shaft pillar and (2) to install instruments near the shaft to monitor shaft stability. Stope instruments provided early data for model validation, calibration, and updating. It was expected that these shaft instruments would then provide objective measurements of ground movement around the shaft in response to pillar mining and would also warn of any potential threat to shaft stability independently of numerical model results.

The initial pillar mining plan was to leave a central 18-m (60-ft) wide pillar within the original 60-m (200-ft) wide shaft pillar. A mechanized cut-and-fill method would be used to mine stopes north and south of the central pillar. The first 5-m (15-ft) high lift was taken below the 3650 level after ramp access was developed. Almost immediately, worrisome indications of ground control difficulties appeared in the form of cracking near the 3200 level, the site of original damage in the 1950's. Concrete slabs in the 3650-level pump room began to crack so that realignment of pipes and pumps became necessary. Some sticking of shaft conveyances occurred.

Although only a small tonnage of ore in the shaft pillar had been mined, the evidence seemed to indicate a serious and growing threat to the Ross shaft. Concerns were expressed by company, union, and regulatory officials. Pillar mining was sharply curtailed while the advice of external consultants was sought. Serious doubts were expressed about the results of the numerical model, which had indicated that the shaft would remain stable after mining the ore reserve 60 m (200 ft) beyond the shaft. However, no plausible explanation was put forth to explain how such a small amount of actual mining [about 9 m (30 ft)] in two lifts) below the 3650 level could produce such severe effects near the 3200 level, which was more than 90 m (300 ft) distant. The need to take some action to ensure the safety of operations led to the definition of two additional "wing" pillars within the original shaft pillar, despite the fact that these pillars would substantially reduce the pillar ore reserve.

Continued research and investigation revealed that long-term creep of the shaft walls[5] had reached the limit of shaft guide adjustment. Thus, sticking of shaft conveyances, although coincidental with the start of pillar mining, was not a direct consequence of taking the first lifts below the 3650 level. Chipping the concrete behind the shaft buntons allowed the buntons to rebound and shaft guide adjustments to be made.

Two hypotheses were advanced to explain the observed damaging effects of stress. One was that graphitic schist, which is weak in shear, or possibly an unknown fault could be causing instability in the shaft. Some exploratory two-dimensional analyses were done in which graphitic schist was represented. A number of effects were obtained by varying the extent, elastic moduli, and strengths of the schist. However, additional site investigations (inspection of drill holes and excavation walls and readings of extensometers installed to monitor stability) did not reveal the presence of a fault or enough graphitic schist to justify incorporating either of these geologic features into the finite-element model. Therefore, it was concluded that the geology was not the source of the observed damage.

The second hypothesis was that the geometry of the two-dimensional model was simply not an adequate approximation of the actual shaft pillar geometry. Two-dimensional (plane strain) analyses are limited (Pariseau and others, 1990). Figure 2 illustrates these limitations. Computer simulations of stope and parallel drift excavation in vertical sections produce horizontal, tunnel-like openings and do not take into account stress concentration about a vertical shaft. No estimate of out-of-plane deformation is possible. Stopes, shafts, and raises excavated in horizontal sections (plan view) produce vertical, shaft-like openings that greatly exaggerate horizontal dis- placements and give no information about vertical motion. Also associated with plane strain analyses is a tacit assumption that the material directions of anisotropic rock, which are associated with foliation strike and dip, coincide with the plane of analysis. Therefore, vertical shear stresses are neglected. Out-of-plane stress and displacement measurements are also not useable for calibration of two-dimensional models.

Because of these limitations and the importance of shafts to mine safety, the feasibility of conducting a three-dimensional, finite-element analysis was investigated. Experience gained in three-dimensional analyses of undercut-and-fill stoping at the Lucky Friday Mine (McMahon and Pariseau, 1989) and of vertical crater retreat mining at the Homestake Mine (Pariseau and Duan, 1989; Pariseau and others, 1989) were quite helpful in addressing the new issues associated with shaft pillar mining.

GEOMECHANICAL MODEL (UTAH3)

Essential requirements of a geomechanical model for simulating shaft pillar mining at the Homestake Mine include (1) elastic behavior to accommodate initial application of load, (2) yielding beyond the elastic limit (elastic-plastic deformation), (3) accommodation of arbitrary initial (pre-excavation) stress states, (4) knowledge of directional rock properties associated with foliation and schistosity (anisotropic elastic moduli and strengths), (5) knowledge of the different rock types and geologic structures, and (6) capability for sequential cuts and fills to follow proposed and historical mining sequences in three dimensions. These requirements were met by a version of the finite-element code UTAH3, which has been in use since 1975 and is similar in concept to UTAH2 (Pariseau, 1978). UTAH2 is now in the public domain (Pariseau and others, 1991), while UTAH3 is not. Of critical importance to implementation of the geomechanics model was an efficient mesh design, one that was reliable and economical.

INPUT DATA

Input data for both codes are similar and include (1) stope geometry and geologic descriptions obtained from mine maps and sections, (2) preexcavation stresses obtained from a number of measurement techniques used in various parts of the mine by several investigators (Johnson and others, 1993), (3) rock and fill properties estimated from laboratory tests and scale factors determined for the shaft pillar region (Pariseau, 1986), and (4) the historical and planned mining sequence.

Rock property scale factors are decimal fractions used to multiply laboratory values of rock properties to obtain rock mass values. A scale factor of 1 implies that the rock mass property of interest is equal to the value determined from laboratory tests. In the absence of prior information, a scale factor of 0.5 may be reasonable (Heuze, 1980). Separate scale factors for elastic moduli and strengths were used in this study. In the two-dimensional analyses described in part 1 of this series (Pariseau and others, 1995a), these were 0.36 and 0.60, respectively, and were obtained by back-analysis, that is, a comparison of measured displacements with model displacements, in conjunction with a simple energy-scaling rule of thumb. This "rule" postulates that strain energy density at failure is independent of scale and requires strengths to be adjusted as the square root of the modulus scale factor. An equally acceptable rule-of-thumb is a strain-to-failure criterion that gives equal modulus and strength scale factors. In any case, the modulus scale factor can be determined from regression analyses of calculated and measured displacement changes in the elastic range.

---

[5] Use of the Ross shaft began December 1934 (Bjorge and others, 1935).

Back-analysis in three dimensions may result in smaller scale factors than would back-analysis in two dimensions because calculated displacements are likely to be less in the former. For example, changes in wall displacement in a circular tunnel are twice those in a sphere of the same diameter excavated in the same material under the same preexcavation hydrostatic stress field (Love, 1944). Consequently, the rock mass modulus needed to bring displacement of a calculated, three-dimensional spherical model into agreement with measured displacement would be one-half that needed to enforce agreement with a two-dimensional cylindrical model. Generally, back-analysis using a three-dimensional model is expected to produce smaller scale factors and lower rock mass moduli and strengths than a two-dimensional model, other factors being equal. A limited parameter study suggested the use of 0.25 and 0.50 for modulus and strength scale factors, respectively, in the three-dimensional analysis of shaft pillar mining at the Homestake Mine. The three-dimensional strength scale factor is five-sixths the two-dimensional factor; both are numerically consistent with the scaling criterion for simple strain energy density.

Geologic information in the form of rock type distribution was part of the input data. Major formations at the Homestake Mine are the Precambrian Poorman Formation in the footwall and the Ellison Formation in the hanging wall. Ore bodies are localized in the Homestake Formation (Slaughter, 1968). This information was incorporated in the model by simply tracing formation contacts as shown on mine sections, which were on 15-m (50-ft) centers. Contact location was subsequently converted to numerical input data using a large digitizing table after the finite-element mesh was developed.

MESH DEVELOPMENT

Mesh development for numerical reliability was governed by several guidelines. The first was that there should be at least five mesh points along the least dimension of a stope or stope combination; the second was that outer mesh dimensions should be at least five times the greatest stope dimension; and the third was that the element aspect ratio should be no greater than five. These guidelines were based on much com- putational experience using an iterative equation solver, which greatly reduces the amount of memory available for fast computations (fast memory). In this regard, UTAH3 requires about 1 kbyte of fast memory per node; a 10,000-node mesh requires about 10 Mbytes of fast memory. A symmetric elimination equation solver using banded storage would require about 50 times as much memory. Fast random access memory (RAM) is not essential, but virtual m e m o r y   g r e a t l y

increases computational time. Overnight turnaround time was desired as a practical matter. Longer times tended to increase the probability of lost runs and reductions in productivity.

Primary stopes at the Homestake Mine were about 15 m (50 ft) wide; the level interval is 46 m (150 ft). These dimensions lead to a minimum mesh width of 230 m (750 ft) with elements about 6 m (20 ft) on edge along the stope walls. There are about 900 elements and 1,700 nodes in a typical vertical section in the shaft pillar region. The entire mesh contains over 34,000 nodes and elements. Figure 3 shows the dimensions of the Ross shaft pillar mesh. The overall mesh was constructed by manually partitioning a generic section through the shaft pillar region, enlarging this section, and then repeating the enlarged section along strike until the outer dimension criterion was met. Figure 3 also shows the main geologic features of the generic section and the mesh refinement used in the proposed pillar mining area. There are 34 element slabs in the mesh.

The central element slab contains the Ross shaft. Figure 4 is a plan view of the mesh in the vicinity of the shaft. The area is about 24 m (80 ft) wide and 30 m (100 ft) long. A more refined "insert" mesh was constructed for this important region. The purpose was to obtain more accurate results in the vicinity of the shaft than allowed for by the larger and "coarser" stope-scale mesh. Inspection of the coarse mesh near the shaft shows elements the size of the shaft itself, which cannot, therefore, indicate localized yielding in the shaft wall. Shaft wall yielding in the coarse mesh would engulf the shaft before the computer model could detect movement. Figure 5 shows the element partitioning of the shaft insert mesh in plan view. The shaded elements in figure 5 define the shaft wall after excavation. There are five nodes along the least dimension of the shaft and more than 5,000 elements in the insert mesh, which extends from top to bottom of the larger coarse mesh. Nodes on the outer boundaries of the shaft insert mesh match companion nodes in the larger coarse mesh.

Procedures simulating a stope lift in pillar mining required running the coarse mesh first and then repeating the same process using the insert mesh. Node displacements from coarse mesh output were then specified as input at the companion nodes of the insert mesh. A means of checking the validity of the procedure is to use a duplicate of the coarse mesh as the insert mesh. Results (element stresses, strains, node displacements) from a given run using the original coarse mesh should agree with the final results using the two-run insert mesh procedure.

Figure 6 illustrates the differences between the shaft wall safety factors obtained with the original coarse mesh and those obtained using the refined insert mesh. The safety factor data in figure 6 refer to rock mass property values, not laboratory

values. The lowest safety factor for the coarse mesh for the shaft wall (about 1.6) was generated after shaft excavation and historical mining but prior to pillar mining. This figure suggested caution. The corresponding insert mesh safety factor was very nearly 1.0 and was a cause for concern. Differences between coarse and insert mesh shaft wall displacements showed a smaller percentage difference than observed in the case of safety factors.

The insert mesh technique has several advantages over a single mesh: less drastic mesh gradation and better numerical performance, smaller size and faster run time, less input and output data. The main use of this technique is for analyses involving openings of greatly different sizes in the same mesh, for example, shafts 4.5 m (15 ft) wide and stopes 45 m (150 ft) wide. The disadvantage is the need to do two runs. Insert meshes may be used in both two- and three-dimensional analyses.

Once the mesh was partitioned into elements, mine sections showing the extent of past mining were overlain at regular intervals along strike of the coarse mesh. Elements occupying old stopes were identified by number and placed in cut element files, which, when sequenced in time, served as historical mining input data. Elements occupying stopes identified in the ore reserve of the Ross shaft pillar were identified in the same way; when sequenced in time, these elements served as pillar mining input data. Stope geometry

is not closely followed during this procedure. A more refined mesh would be required if accurate stress concentration measurements in the stope walls were needed.

Computer run times per cut in the 34,000-node coarse mesh ranged from several days using the virtual memory capability of a Prime computer to about an hour on an IBM 3090 to a few minutes using a Cray X-MP machine. Workstation (HP 9000) run times were two to three times longer, about 2 to 3 h, than IBM 3090 run times.

MODEL VERIFICATION

Comparisons between the two-dimensional code UTAH2 and the three-dimensional code UTAH3 were done to verify the three-dimensional model and to establish confidence in the consistency of results. The main procedure used a transitional tunnel problem in which a tunnel-like opening was excavated in an initially stressed rock mass (1) in a plane strain analysis using UTAH2, (2) in a single-element slab using UTAH3, and (3) end-to-end in the coarse mesh using UTAH3. No displacement of the outer mesh faces perpendicular to the tunnel axis was allowed in the three-dimensional meshes. Figure 7 compares the stresses in the elements composing the tunnel walls. The results from the three-dimensional analyses are in close agreement with results from the two-dimensional analysis, which verifies procedural and code consistency.

FINITE-ELEMENT MODEL CALIBRATION

In principle, the calibration procedure for the three-dimensional Ross shaft pillar model was the same as for the earlier two-dimensional model. Regression analyses of calculated and measured displacements obtained within the elastic range of deformation provided a scale factor for elastic moduli. Extent of yielding beyond the elastic limit served to identify a strength scale factor. The same scale factor for elastic properties was applied to all elastic moduli; similarly, the same scale factor for strength was applied to all strengths (Pariseau and others, 1985). Rock mass properties for use in the calibrated model were then obtained by multiplying laboratory test values of moduli and strengths by the appropriate scale factor. Model calibration also depended on the preexcavation stress state, which then required verification for complete model calibration.

ROCK PROPERTIES

The finite-element code UTAH3 allows for independent anisotropic elastic and strength properties. The anisotropy allowed provides for three mutually orthogonal material axes,

that is, orthotropic rock properties. A generalized Hooke's law relates stress and strain in the elastic range of deformation. Quadratic, pressure-dependent yield criteria limit the range of purely elastic deformation (Pariseau, 1972). Associated flow rules are used in the postelastic range. Each of the three major formations at the Homestake Mine (Poorman, Homestake, and Ellison) thus require nine independently specified elastic moduli and strengths; 54 are required in all. Laboratory test values are given in part 1 of this series (Pariseau and others, 1995a). Some igneous dikes occur in the shaft pillar region; these were assigned properties appropriate to the Homestake Formation. Old stopes are filled with sand and waste rock. Properties for these materials were assumed to be isotropic and were estimated on the basis of experience. Both had negligible influence on shaft stability.

PREEXCAVATION STRESSES

The preexcavation stress state before the first underground mining was done at the Homestake Mine was characterized by normal stress factors σ_v (vertical stress), σ_H (stress

perpendicular to strike), and σ_h (stress parallel to strike) in kilopascals. In this analysis, $\sigma_v = 28.275$ Z, $\sigma_H = 14,317 + 11.99$ Z, and $\sigma_h = 834 + 12.44$ Z. Z is depth below the surface in meters.

This characterization was obtained from several stress measurements taken in different sections of the mine by different investigators using borehole deformation gauges and doorstopper cells. Stress measurements were also made using hollow inclusion and borehole deformation gauges in the course of the current shaft pillar study. These data pertain to the stress state that existed after much historical mining but prior to any shaft pillar mining. A similar set of stresses was calculated through a finite-element simulation of historical mining that included sinking of the Ross shaft in an unperturbed stress field but with no pillar mining.

The finite-element simulation of historical mining used the figures above as initial stresses. Initial normal stresses (preexcavation) and posthistorical normal stresses (prepillar mining) are shown in table 2. Generally, shear stresses were an order of magnitude less than normal stresses. Additional details are given in Johnson and others (1993). The data in table 2 show that the finite-element stresses were higher than the measured stresses on the 3650 level of the shaft pillar prior to pillar mining. Higher prepillar mining stresses were expected to induce higher postpillar model stresses and thus to introduce some conservatism in the analysis. Additional adjustments to scale factors and initial stresses for model calibration were not justified because of uncertainties in the data, which included large variations in stress measurements (20% to 40% above and below mean values) and the assumption of isotropy in stress measurements.

Table 2.—Preexcavation and posthistorical mining stresses, kilopascals

	North-south, σ_h	East-west, σ_H	Vertical
Preexcavation	14,700	27,700	31,500
Posthistorical:			
Measured	16,300	25,600	28,700
Model	17,800	33,700	42,300

DISPLACEMENT DATA

Displacement data for model calibration were obtained from multipoint borehole extensometers (MPBX's) installed near shaft and stope walls (figure 8). Shaft extensometer displacements were generally small, a few millimeters. Figure 9A is an example of shaft extensometer response over a 3-year period following installation in November 1987. Positive displacement indicates e x t e n s i o n relative to the collar.

Remote extensometers extended away from the shaft pillar into undisturbed ground where little motion was expected. Displacement data shown in figure 9A confirm this expectation.

Stope extensometers were installed in the vicinity of first pillar mining to obtain calibration data early in the life of the project. Stope extensometers generally produced large displacements, more than 10 mm (0.4 in), and were first used to calibrate the two-dimensional model (Pariseau and others, 1995b). Figure 9B shows a recording of an extensometer installed in a cross-cut rib near a stope on the 3650 level where pillar mining began. In this regard, stope extensometer installation preceded pillar mining by several months. The response of the hanging wall stope extensometer was similar to that shown in figure 9B and included large step-like increases over a period of several months before reaching the recording limits of the instruments (Pariseau and others, 1995b).

Both types of extensometer data illustrated in figure 9 show relatively large displacements that were common to all points on a given extensometer. At the same time, relative dis- placements between points of a given extensometer were much smaller. For example, the stope data in figure 9B show about 36 mm (1.4 in) of common displacement but only about 3 mm (0.1 in) of relative displacement between points along the instrument hole. This phenomenon is most simply explained by motion of the reference point at the hole collar that, in turn, is associated with yielding of the cross-cut wall in the neighborhood of the hole collar. Indeed, cracking and sloughing of development walls near stopes was not unusual or unexpected. The common displacement in shaft extenso- meter data and motion of the shaft extensometer collars are less easily explained because there was little visual evidence of yielding. Creep was indicated, but whether associated with the rock mass, with extensometer cement, with other aspects of installation, or some combination is unknown. The example data in figure 9 are the best available; many plots defied interpretation and much of the data were lost because of power stoppages, equipment failures, electrical noise, and so forth.

Extensometer output allows for direct conversion into measurements of relative displacement between anchor points located at regular intervals along the instrument hole and the hole collar point. A positive relative displacement indicates elongation parallel to the hole. Finite-element simulation of the mining sequence allows for calculation of relative displacements that correspond to the measured displacements. Only displacements that occurred after installation of an extensometer were used in the calculated "readings." The finite-element simulation sequences of historical and shaft pillar mining are given in table 3.

Table 3.—Historical and shaft pillar mining sequences

Cut number	Mining simulation
Historical sequence (past mining north and south of shaft pillar):	
1	Sinking of the Ross shaft.
2	Stoping below 3650 level.
3	Stoping between 3650 and 3500 levels.
4	Stoping between 3500 and 3350 levels.
5	Stoping between 3300 and 3250 levels.
6	Stoping above 3250 level.
Pillar mining (calibration and updating sequence):	
7	Excavation 3650 hanging wall drift, November 1987.
8	June 1988.
9	July 1988.
10	December 1988.
11	February 1989.
12	April 1989.
13	May 1, 1989.
14	May 10, 1989.
Pillar mining (further updates, including north and south of central pillar):	
15	July 1989.
16	October 1990.
17	November 1992.
18	December 1992.
19	January 1994.
20	August 1994.
Pillar mining (future central pillar extraction):	
21	Estimated summer 1995, 3650 level sill to +50.
22	Estimated winter 1995, 3650 level, +50 to +100.
23	Estimated summer 1996, to 3500 level.
24	Estimated winter 1996, 3500 level sill to +50.
25	Estimated summer 1997, 3500 level, +50 to +100.
26	Estimated winter 1997, to 3350 level.

REGRESSION ANALYSES

Elastic behavior allowed for regression analyses using a linear model. The regression variables were calculated displacements (y-axis) on measured displacements (x-axis). The slope of the regression line is the ratio of Young's modulus associated with measured displacements to the modulus used in the finite-element calculations, provided that the rock mass behavior is entirely elastic. This ratio is, in fact, an elastic modulus scale factor. Inelastic behavior in the mine and in the model introduce some degree of nonlinearity. The square of the correlation coefficient (r^2) is a measure of the variance that may be explained by a simple, linear model; a correlation coefficient (r) greater than 0.71 explains more than 50% of the data variance. Unfortunately, very few case histories in rock mechanics compare calculated with measured displacements, so there is no large body of evidence nor consensus of expert opinion as to what may be considered a reliable fit of model results to mine measurements. A correlation coefficient of 0.7 or higher may be considered a satisfactory fit, especially in view of the effects of inelastic phenomena about many mine openings. Regression analyses thus provide guidance toward determining an appropriate scale factor for model calibration, but such analyses are not absolute.

Table 4 shows the results of several regression analyses of calculated extensometer displacements on measured displacements. These displacements are relative between extensometer points in both model and mine data and are accumulated differences between the time of installation

Table 4.—Regression analysis of calculated extensometer displacements on measured displacements

Line Number	Extensometers used in regression analysis		Number of data points	Regression line slope	Regression line intercept	Regression correlation coefficient r	Maximum measured displacement, mm	Maximum calculated displacement, mm	Extensometer lengths, m
	Type	Number							
1	Shaft	E3	27	0.84	0.01	0.96	3	3	30
2	Shaft	E1, E9, E10	81	0.25	0.00	0.65	2	0.5	30, 60
3	Stope	E14, E17, E18	17	2.43	0.07	0.74	6	20	18
4	Combination of 2 and 3	E1, E9, E10, E14, E17, E18	98	2.68	−0.02	0.81	6	20	18, 30, 60
5	Combination of 1, 2, and 3	E1-E3, E9, E10, E14, E17, E18	152	1.90	−0.01	0.71	6	20	18, 30, 60
6	Combination of 1 through 5	E1-E3, E7-E10, E14, E17, E18	206	1.78	0.00	0.68	6	20	18, 30, 60

and pillar stoping time. Displacement changes were calculated in accordance with the mining sequences in table 3, beginning with the historical sequence and proceeding through the pillar mining calibration sequence. The number of points in table 4 was determined by the number of pillar mining steps, the number of extensometers, and the number of anchor points per extensometer.

The shaft extensometer regression data in line 1 of table 4 shows a very high correlation coefficient (r = 0.96) and a regression line slope of 0.84, which suggests that a somewhat lower modulus scale factor should be used (84% of the input 0.25 modulus scale factor). However, the shaft extensometer regression in line 2, which has a lower correlation coefficient (r = 0.65) but which is based on many more data points, suggests a much lower scale factor. The shaft displacement data in both lines 1 and 2 show a maximum displacement of about 3 mm (0.1 in) over lengths of 30 to 60 m (100 to 200 ft), that is, less than one part in ten thousand, which is a uniaxial strain equivalent of 0.01%.

The stope extensometer regression in line 3 shows much larger displacements. Calculated displacements reach 20 mm (0.8 in) over a length of 18 m (60 ft), which amounts to roughly one part in one thousand, or about 0.1% uniaxial strain equivalent. The correlation coefficient (r = 0.74) is in the satisfactory range, but the calculated displacements are much larger than those measured. This overestimation is reflected in the regression line slope of 2.43, which indicates that the input scale factor of 0.25 should be increased by 143%, to 0.61.

Combinations of shaft and stope extensometer regressions are shown in lines 4, 5, and 6 using an increasing number of data point pairs (98 to 206). The regression line slopes decrease from 2.68 to 1.78, indicating a modulus scale factor ranging from 0.67 to 0.45. The correlation coefficient decreases from 0.81 to 0.68.

These results suggest a modulus scale factor that is equal to the strength scale factor (0.50). The results also suggest that the alternative strain-to-failure criterion may be applicable. However, the case is not clear because there is no guarantee that the only points in the elastic domain are present in the data. Overestimated (model) displacements may result from rock mass model strengths that are too high, as well as elastic moduli that are too low. In addition, experience with extensometer data shows that the goodness of fit indicated by the correlation coefficient may be influenced by the magnitudes of the measured displacements (Pariseau and Duan, 1989). Figure 10 shows such an effect in data obtained from an earlier study of vertical crater retreat mining at the Homestake Mine (Pariseau, 1986). Inspection of figure 10 shows that displacements greater than about 2 mm (0.08 in) are needed to achieve a correlation coefficient greater than 0.70. Smaller displacements lead to low correlation coefficients. The same phenomenon appears in the shaft pillar data; large stope displacements lead to high correlation coefficients, while the smaller shaft displacements are not well correlated. Thus, as a practical matter, much of the rather small amount of displacement from the shaft extensometers may simply be noise. Despite such complications, some justification for an increase in the elastic properties scale factor could be made.

An accurate, independent determination of rock mass strength would help to clarify the situation. However, the nonlinearity introduced by yielding in the model and in the mine pose substantial analytical difficulties that remain to be resolved. The strength scale of 0.5 adopted for the Ross shaft pillar project was based on (1) the extent of yielding inferred between the stope hanging wall and the development drift on the 3650 level during calibration of the two-dimensional model (Pariseau and others, 1995b) and (2) a simple analytical relationship between two- and three-dimensional back-analyses of long cylindrical and spherical excavations. Although better fits of the model results to mine measurements were desired, correlation coefficients of about 0.7 were considered satisfactory for the initial calibration of the three-dimensional shaft pillar model. Thus, scale factors of 0.25 and 0.50 for elastic moduli and strengths were adopted for the Ross shaft pillar model.

APPLICATION OF THE CALIBRATED MODEL

The most important application of the calibrated model was an assessment of shaft stability with respect to the effects of pillar mining. The model was also applied to the functioning of the two horizontal wing pillars in the main shaft pillar, the role of the central pillar, and potential deformation of shaft framing. Figure 11*A* shows the central pillar in a plan view of the 3650 level; figure 11*B* shows the wing pillars in a vertical east-west section through the original shaft pillar. Ex- tensometer readings expected at various stages of future pillar mining were calculated in advance to detect any substantial departure from model forecasts as pillar mining proceeded.

Safety factor distributions and changes in safety factor induced by various pillar mining sequences were the most important tools for interpreting model results in terms of shaft stability. Direct model output in the form of numerical values of displacements, strains, and stresses induced by mining are not directly associated with objective criteria of stability. The

safety factor actually used for stability assessment was the ratio of strength to stress, where strength is stress at the limit of elastic deformation. Any tendency to increase stress beyond the elastic limit would result in inelastic yielding, that is, elastic-plastic deformation.

Specifically, the yield condition (Y) that marks the limit to purely elastic deformation is $Y = J^{(n/2)} + I$, where n = 2 in the present analysis, J = an anisotropic expression that reduces to a dimensionless second invariant of deviatoric stress in the isotropic case, and I = an anisotropic form that reduces to a dimensionless first invariant of stress in the isotropic case (Pariseau, 1972). When n = 1 and isotropy prevails, one obtains the Drucker-Prager yield condition. The isotropic form of the yield condition has a parabolic shape (n = 2) in principal stress space and depends on all three principal stresses. No assumption is necessary concerning the direction or magnitude of the intermediate principal stress, which is often the case in many two-dimensional models based on the Mohr-Coulomb criterion. This is the same yield condition that was used in the two-dimensional model (Pariseau and others, 1995a; 1995b). When the elastic limit is reached, Y = 1. The greatest value of $(J)^{1/2}$ possible is thus $(J)^{1/2}_{max} = (1 - I)^{-n}$, which depends on element stresses. The actual value is $(J)^{1/2}_{act}$, which also depends on the element stress state. The element safety factor is then the ratio of $(J)^{1/2}_{max}$ to $(J)^{1/2}_{act}$. Uniaxial compressive, tensile, and shear failures are special cases that may arise in response to the evolving element stresses; they are handled automatically during the model run.

Structural criteria for shaft bunton safety were not developed, but a simple calculation shows that a 6-mm (0.25-in) axial compression of a 6-m (20-ft) long mild steel beam causes the stress to reach the elastic limit. This calculation suggests that shaft wall closure greater than 6 mm (0.25 in) may result in structural damage to shaft framing. Of course, actual shaft wall motion is a complex, three-dimensional phenomenon and varies in time as mining proceeds. The accuracy required to use finite elements to predict structural damage was considered beyond the accuracy of the geomechanics model. Model results did indicate several centimeters of shaft wall displacement. However, the relative displacements between opposing shaft walls were much smaller. The opening appeared to "float" with the rock mass in response to historical and pillar mining.

SHAFT STABILITY

The Ross shaft was considered safe and stable with respect to large, possibly catastrophic, ground motions if shaft wall deformations induced by mining in the shaft pillar remained in the elastic range. Yielding, if present, could not encompass the shaft. Some localized yielding in the skin of an opening could be tolerated because such yielding could be controlled easily by bolting, screening, or other conventional ground-control measures. These safety and stability criteria were met

in the first three-dimensional, finite-element simulations of historical and planned pillar mining that called for a central pillar and two horizontal wing pillars to be left within the main shaft pillar.

The distribution of the shaft wall safety factor as a function of depth at various stages of mining is shown in figure 12. In this regard, the shaft wall safety factor is the *lowest* factor of safety in any element at the shaft wall. This element (27) tended to be the same regardless of depth and is identified in the insert mesh illustrated in figure 5. Figure 12 shows that most of the change in the shaft wall safety factor had occurred in association with historical mining. Simulation of the original pillar mining plan, in which the central pillar and the two wing pillars were left, showed little change subsequent to historical mining. Nowhere along the shaft route did the safety factor become less than about 1.0; the shaft wall remained in elastic ground.

As determined by the shaft wall motions, model results are illustrated in figure 13. The bulges in figure 13 draw attention to the influence of pillar mining on shaft wall position.

WING PILLARS

The two wing pillars accounted for about 25% of the original shaft pillar ore reserve. The wing pillars were introduced into the pillar extraction plan shortly after the first lifts were taken below the 3650 level. At that time, cracking was again initiated near the site of original shaft damage on the 3200 level and in the pump room on the 3650 level. No three-dimensional model results were available for design guidance at the time.

Subsequent development of the three-dimensional model and simulation of alternative shaft pillar mining sequences in which the wing pillars were recovered showed few differences in safety factor when compared with sequences in which the wing pillars were left. As before, most of the changes in safety factors in the shaft wall occurred with historical mining; pillar mining induced only a small change, and the wing pillars had little effect.

The fact that model results continued to show that observed ground motion and extensometer readings were within expectations gave credibility to the suggestion that the wing pillars were not needed to ensure shaft stability. This result was timely enough to be incorporated into the decision to extract the upper, second wing pillar and to recover the lower wing pillar at a future date.

CENTRAL PILLAR

The decision to create a central pillar was based on a premining analysis of a two-dimensional plan view that involved simulation of historical mining north and south of the original 60-m (200-ft) wide shaft pillar followed by simulations of various shaft pillar mining sequences.

Extraction of the full width of the original shaft pillar immediately west of the Ross shaft produced large displacements at the shaft walls. The central pillar reduced shaft wall displacements associated with pillar mining to about 9.5 mm from 24.1 mm (0.38 in from 0.95 in) or about 60% in simulations using an 18-m (60-ft) central pillar. The central pillar was introduced into the original pillar extraction plan from the outset and also accounted for about 25% of the total ore reserve.

A plan was developed to extract the central pillar following recovery of the ore reserves in the shaft pillar. Mining would proceed from the lower levels upward using mechanized cut-and-fill methods as before. The geomechanics model would be recalibrated at the same time existing stope instruments were repaired and new instruments installed. Extensometers would be used to measure pillar displacements induced by mining on either side of the central pillar between the 3650 and 3350 levels.

Unfortunately, operational demands prevented implementation of the plan before the stopes on either side of the central pillar had been completed. Consequently, mining of the central pillar had to be simulated using the scale factors for the original rock properties, that is, 0.25 and 0.50 for elastic moduli and strengths, respectively. The simulations were carried out before the first lift was taken in the central pillar. Table 3 shows run number and cut, beginning with the original Ross shaft cut (CT1), proceeding through historical mining (CT6) and pillar mining on the north and south sides of the central pillar (CT20), and through mining the central pillar (CT26).

Figure 14 shows the distribution of the shaft wall safety factor at the end of the Ross shaft cut (CT1), at the end of historical mining (CT6), just before the central pillar was mined (CT20), and after the central pillar was extracted (CT26). Most of the decrease in safety factor occurred in conjunction with historical mining. Stress relief associated with pillar mining actually increased shaft wall safety factors between the 3200 and 3650 levels. Below the 3650 level, a small additional decrease occurred. This decrease was enough to cause some shaft wall elements to respond inelastically as

the safety factor was reduced to 1. Figure 15 shows that the calculated yield zone was confined to elements at the shaft wall and was limited to a few elements near the shaft corners.

Although absolute displacement of the shaft wall is not a reliable index to stability, displacement calculations assist in visualizing shaft wall motions and provide a basis for estimating what extensometer readings will be. The major component of shaft wall displacement is toward the pillar mining region, that is, in an east-west direction. Figure 16 shows calculated east-west displacement of the southeast corner of the shaft wall. The negative displacement in figure 16 is westward toward pillar mining. Each mining phase results in additional displacement, that is, historical mining resulted in about 1 cm (0.5 in) of displacement, pillar mining roughly doubled shaft wall displacement, and simulation of central pillar mining indicated an additional 1 cm (0.5 in) of shaft wall displacement.

Mining-induced shaft displacements will be superposed on long-term creep and will eventually require adjustment of shaft guides to ensure that conveyances will operate smoothly. The exact timing is uncertain, but it can be estimated by monitoring and inspection.

SHAFT FRAMING

Relative displacements between shaft walls provide a measure of shaft deformation that may be transmitted to shaft buntons and other frame components. Shaft strains were defined as relative displacements per unit of shaft dimension (width and breadth in a horizontal plane). Figure 17 shows these strains as a function of depth after the shaft cut, at the end of historical mining, before central pillar mining, and at the end of central pillar mining (CT1, CT6, CT20, and CT26, respectively). Figure 17 also shows that the greatest compressive strain, 300 microstrain, is associated with historical mining, whereas an extension strain of 500 microstrain is shown at the end of simulated central pillar mining. These estimated deformations are below an elastic limit of steel, for example, 1,000 microstrain.

DISCUSSION

Repeated analyses using different combinations of elastic moduli and strength scale factors might lead to a better overall fit of model displacements and yield zones to extensometer readings and yield zones actually seen in development openings and stope walls. More elaborate back-analyses that include the preexcavation stress state could also be done for the purpose of achieving better agreement with mine

measurements and observations. However, the computational effort would be enormous, and there is no guarantee that the results would be much different or more reliable. In this regard, the more general back-analysis procedures (including the inverse characterization problem, as well as the direct approach used here) are reviewed by Gioda (1985), who points out that "it is impossible to carry out a meaningful

calibration if the values of the measured data are too close to the tolerance of the measuring device." Gioda also notes that "a careful choice of the type of quantity to be measured and the locations where the measurements are performed" is essential. In this regard, the resolution of an extensometer may be a fraction of a millimeter in the laboratory, but in mining practice, sensitivity appears to be much less.

The three-dimensional geometry and geology of hard-rock mines continues to defy rapid preparation of meshes and easy visualization of results. While increased storage capacity and speed of computer hardware makes 24-h turnaround time feasible for medium-scale finite-element meshes ($\approx$30,000 nodes), advances in low-cost, user-friendly meshing and visualization tools remain a pressing need.

CONCLUSION

In conclusion, this study has demonstrated, through an integrated program of laboratory testing, stress analysis, and mine measurements, that three-dimensional, finite-element analysis is an engineering tool for mine stability analyses

and design where the cost is justified by the importance of the mining objective, in this case, the safe and profitable recovery of ore in shaft pillars.

ACKNOWLEDGMENTS

REFERENCES

Bjorge, G. N., A. J. M. Ross, J. D. Johnson, S. J. Staple, and J. F. Wiggert. Construction and Equipment of the Ross Shaft, Homestake Mining Company. AIME Tech. Publ. 621, Class A, Metal Mining, No. 57, 1935, 43 pp.

Gioda, G. Some Remarks on Back Analysis and Characterization Problems in Geomechanics. Paper in Numerical Methods in Geomechanics, Nagoya 1985: Proceedings of the Fifth International Conference, ed. by T. Kawamoto and Y. Ichikawa (Nagoya, Japan, Apr. 1-5, 1985). Balkema, v. 1, 1985, pp. 47-61.

Heuze, F. E. Scale Effects in the Determination of Rock Mass Strength and Deformability. Rock Mech., v. 12, No. 3-4, Mar. 1980, pp. 167-192.

Johnson, J. C., W. G. Pariseau, D. F. Scott, and F. M. Jenkins. In Situ Stress Measurements Near the Ross Shaft Pillar, Homestake Mine, SD. USBM RI 9446, 1993, 17 pp.

Love, A. E. H. A Treatise on the Mathematical Theory of Elasticity. Dover, 1944, pp. 142-144.

McMahon, T., and W. G. Pariseau. A Comparison Between Two- and Three-Dimensional Numerical Models of a Coeur d'Alene District Mine. Paper in Rock Mechanics as a Guide for Efficient Utilization of Natural Resources: Proceedings of the 30th U.S. Symposium, ed. by A. W. Khair (WV Univ., Morgantown, WV, June 19-22, 1989). Balkema, 1989, pp. 963-970.

Pariseau, W. G. Interpretation of Rock Mechanics Data (contract HO220077, Univ. of UT). USBM OFR-47(2)-80, v. 2, 1978, 41 pp.

Pariseau, W. G. Plasticity Theory for Anisotropic Rocks and Soils. Paper in Basic and Applied Rock Mechanics, 10th Symposium on Rock Mechanics (Univ. TX at Austin, 1968). Soc. Min. Eng., AIME, 1972, pp. 267-295.

Pariseau, W. G. Research Study on Pillar Design for Vertical Crater Retreat (VCR) Mining (contract JO215043, Univ. of UT). USBM OFR 44-86, 1986, 232 pp.; NTIS PB 86-210960.

Pariseau, W. G., E. L. Corp, and M. E. Poad. Recent Experience in Calibration of Finite-Element Models by Back Analysis of Underground

Hardrock Mine Data. Paper in Proceedings International Symposium on Large-Scale Underground Mining (Univ. of Lulea, Sweden). 1985, pp. 175-182.

Pariseau, W. G., and F. Duan. Finite-Element Analyses of the Homestake Mine's Study Stope: An Update. Paper in Numerical Models in Geomechanics—NUMLOG III, ed. by S. Pietruszczak and G.N. Pande (Niagara Falls, ON, May 8-11, 1989). Elsevier, 1989, pp. 566-576.

Pariseau, W. G., J. C. Johnson, M. M. McDonald, and M. E. Poad. Rock Mechanics Study of Shaft Stability and Pillar Mining, Homestake Mine, Lead, SD (In Three Parts): 1. Premining Geomechanical Modeling Using UTAH2. USBM RI 9531, 1995a, 20 pp.

_____. Rock Mechanics Study of Shaft Stability and Pillar Mining, Homestake Mine, Lead, SD (In Three Parts): 2. Mine Measurements and Confirmation of Premining Results. USBM RI 9576, 1995b, 13 pp.

Pariseau, W. G., J. C. Johnson, and S. Orr. Three-Dimensional Analysis of a Shaft Pillar at the Homestake Mine. Paper in Rock Mechanics Contributions and Challenges: Proceedings of the 31st U.S. Symposium, ed. by W. A. Hustrulid and G. A. Johnson (CO Sch. Mines, Golden, CO, June 18-20, 1990). Balkema, 1990, pp. 529-536.

Pariseau, W. G., M. M. Mcdonald, J. C. Johnson, and M. E. Poad. Personal Computer Finite-Element Modeling for Ground Control and Mine Design. Pres. at USBM workshop, March 1, 1991, 42 pp. + appendices; available from J. C. Johnson, Spokane Research Center, Spokane, WA.

Pariseau, W. G., M. Poad, and E. L. Corp. Extended Three-Dimensional Finite Element Analyses of the Homestake Mine Study Stope. Paper in Rock at Great Depth: Rock Mechanics and Rock Physics at Great Depth, ed. by V. Maury and D. Fourmaintraux. V. 1, Balkema, 1989, pp. 733-738.

Slaughter, A. L. The Homestake Mine. Ch. in Ore Deposits in the United States, 1933-1967, ed. by J. D. Ridge. V. 2, AIME, 1968, pp. 1336-1459.
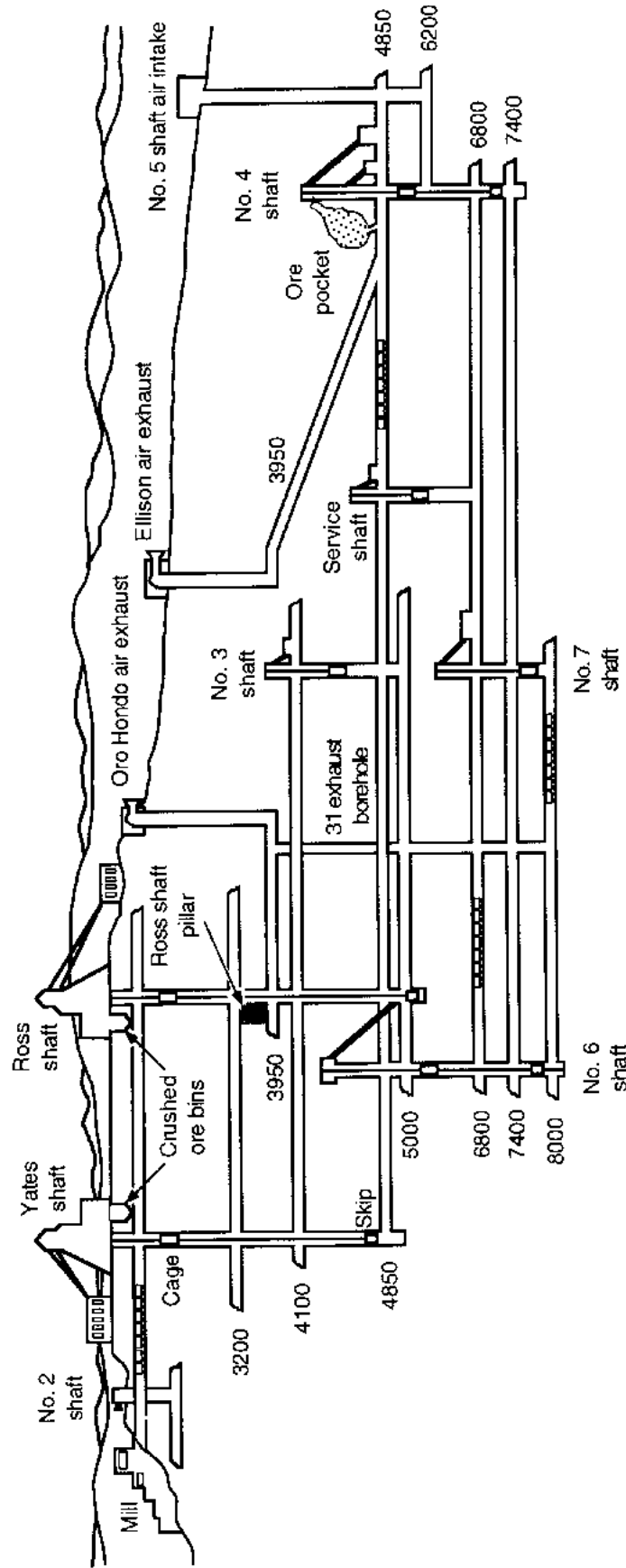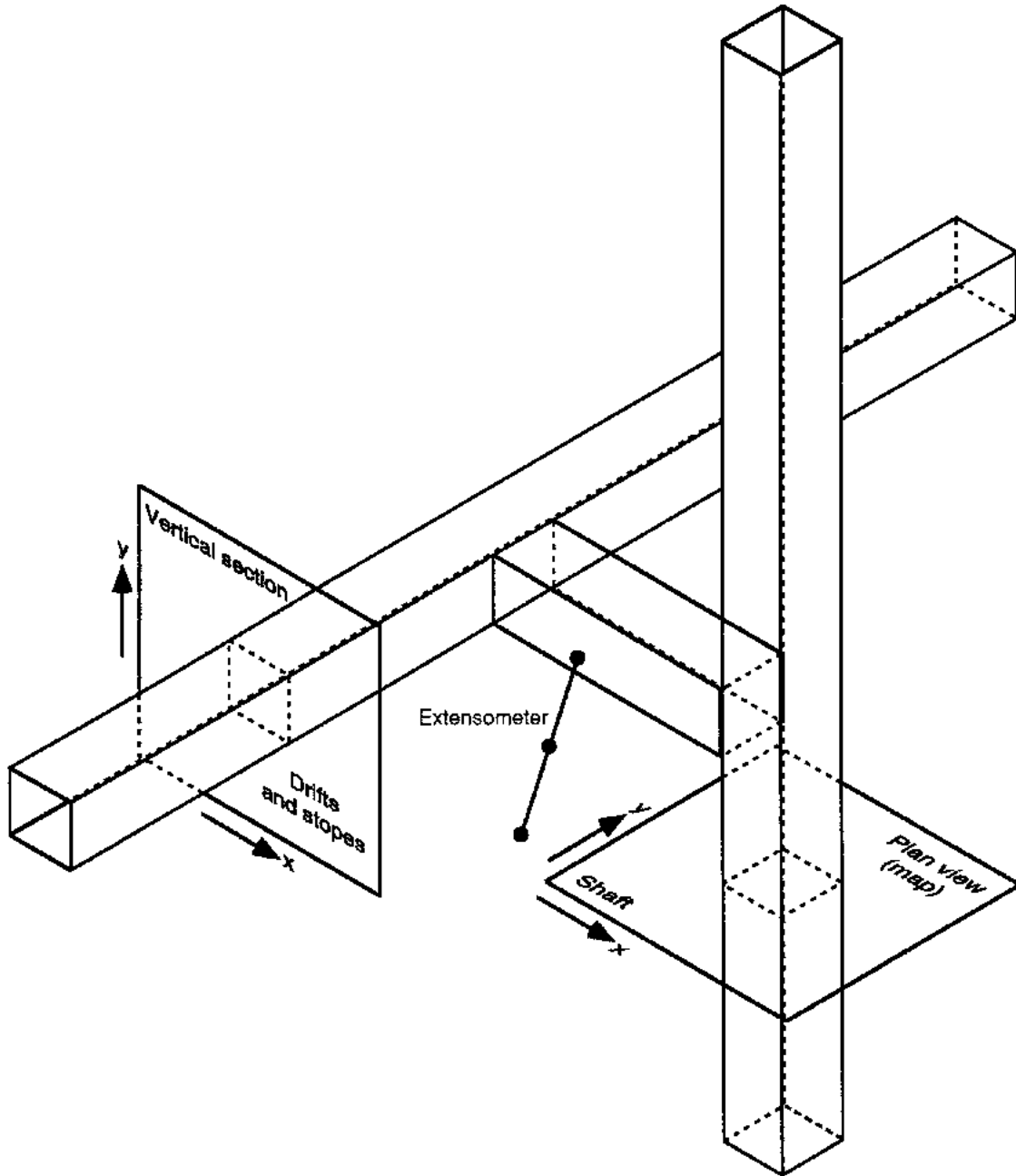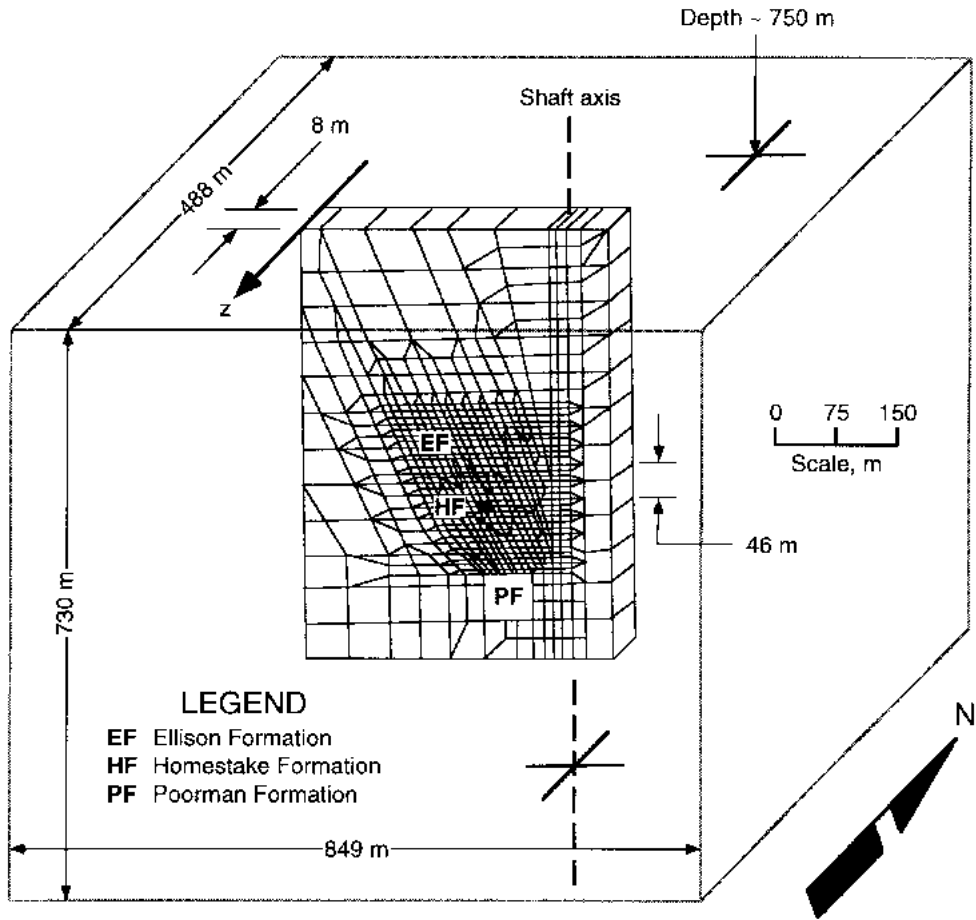
12

Figure 1

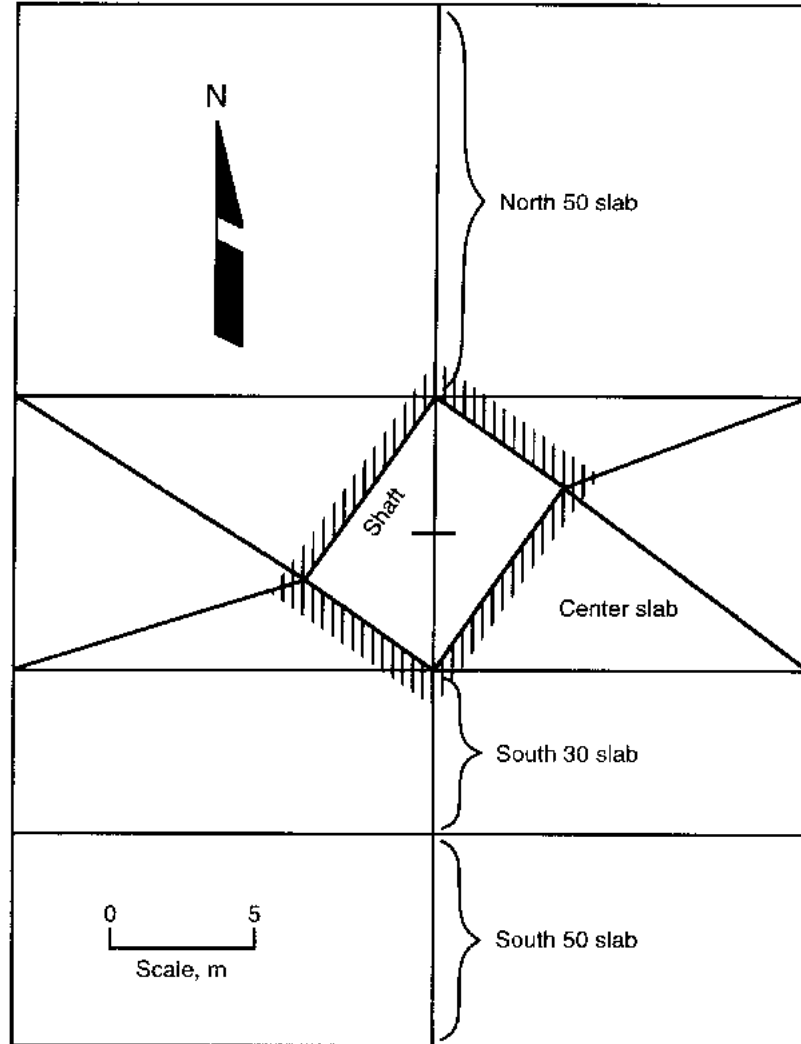*Homestake Mine development*

Figure 2

Section and plan views of two-dimensional models.
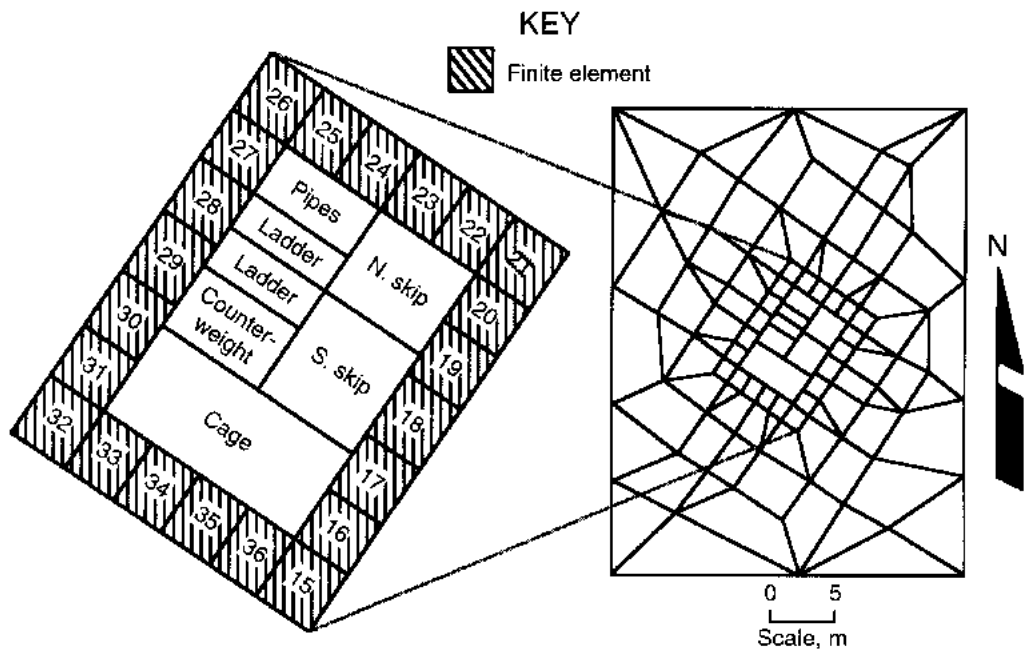
14

Figure 3

Three-dimensional, finite-element mesh.
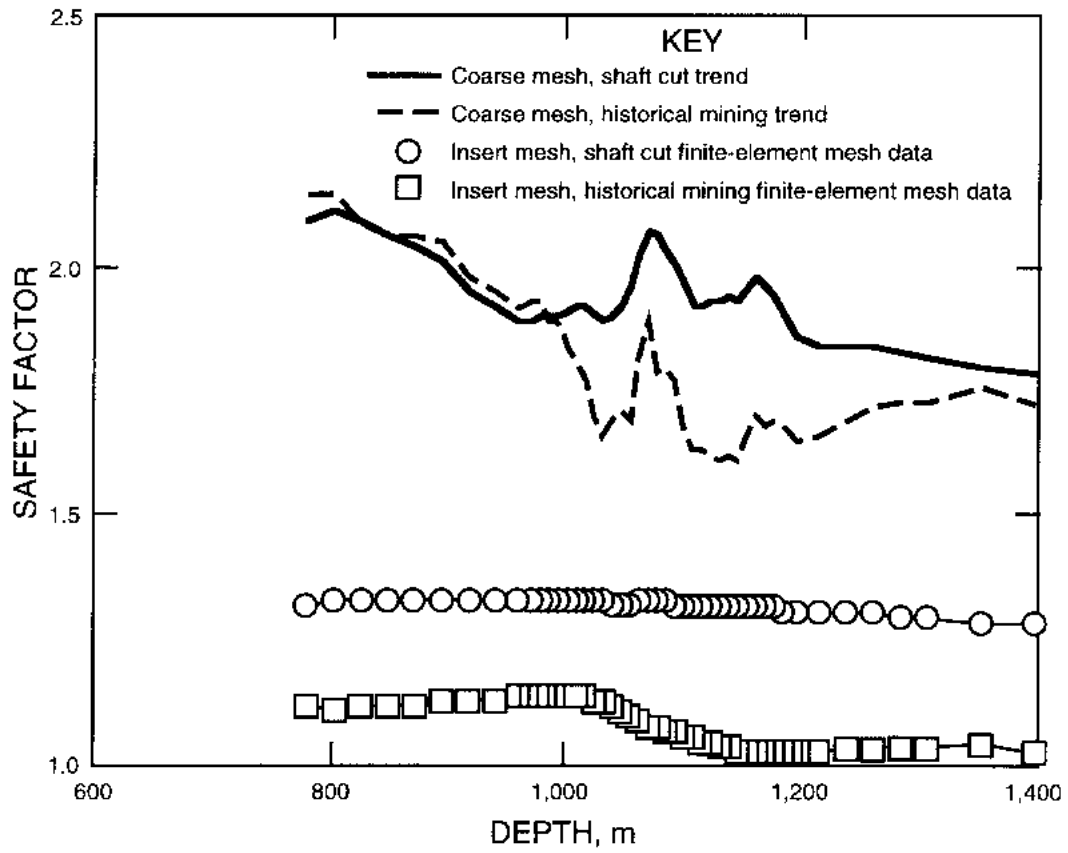
Figure 4

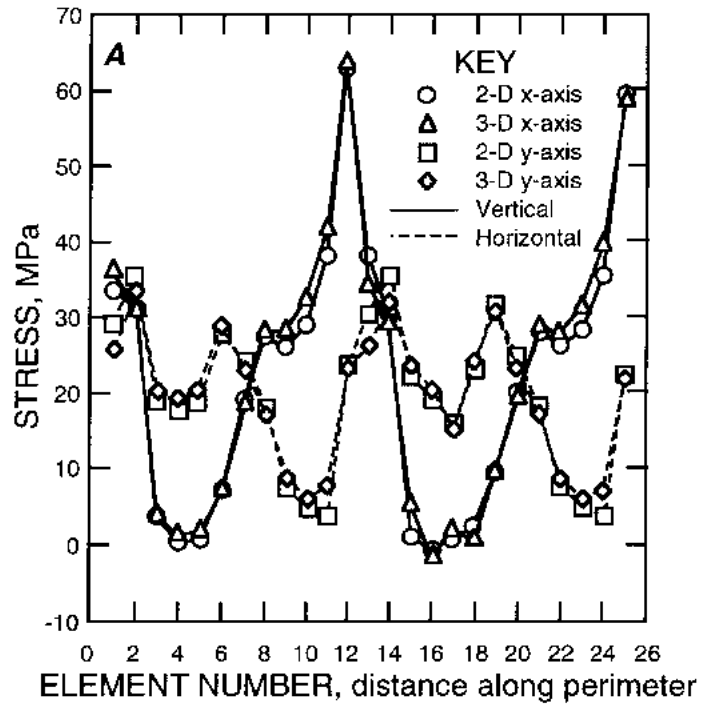*Plan view of coarse mesh about shaft.*

16

Figure 5

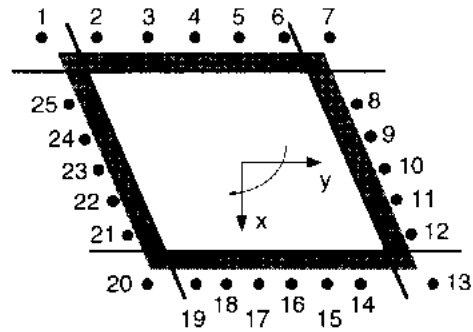*Plan view of insert mesh about shaft.*

Figure 6

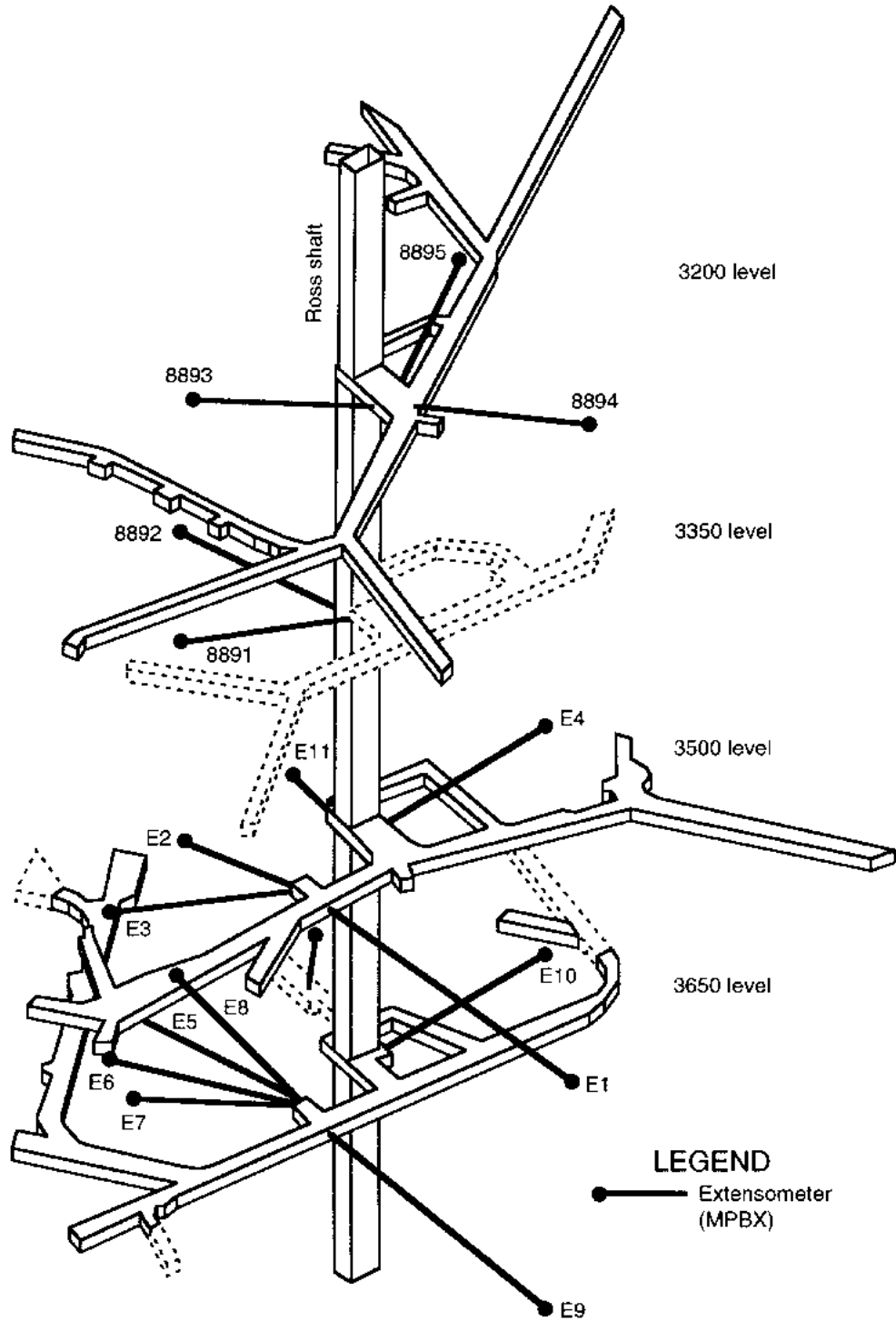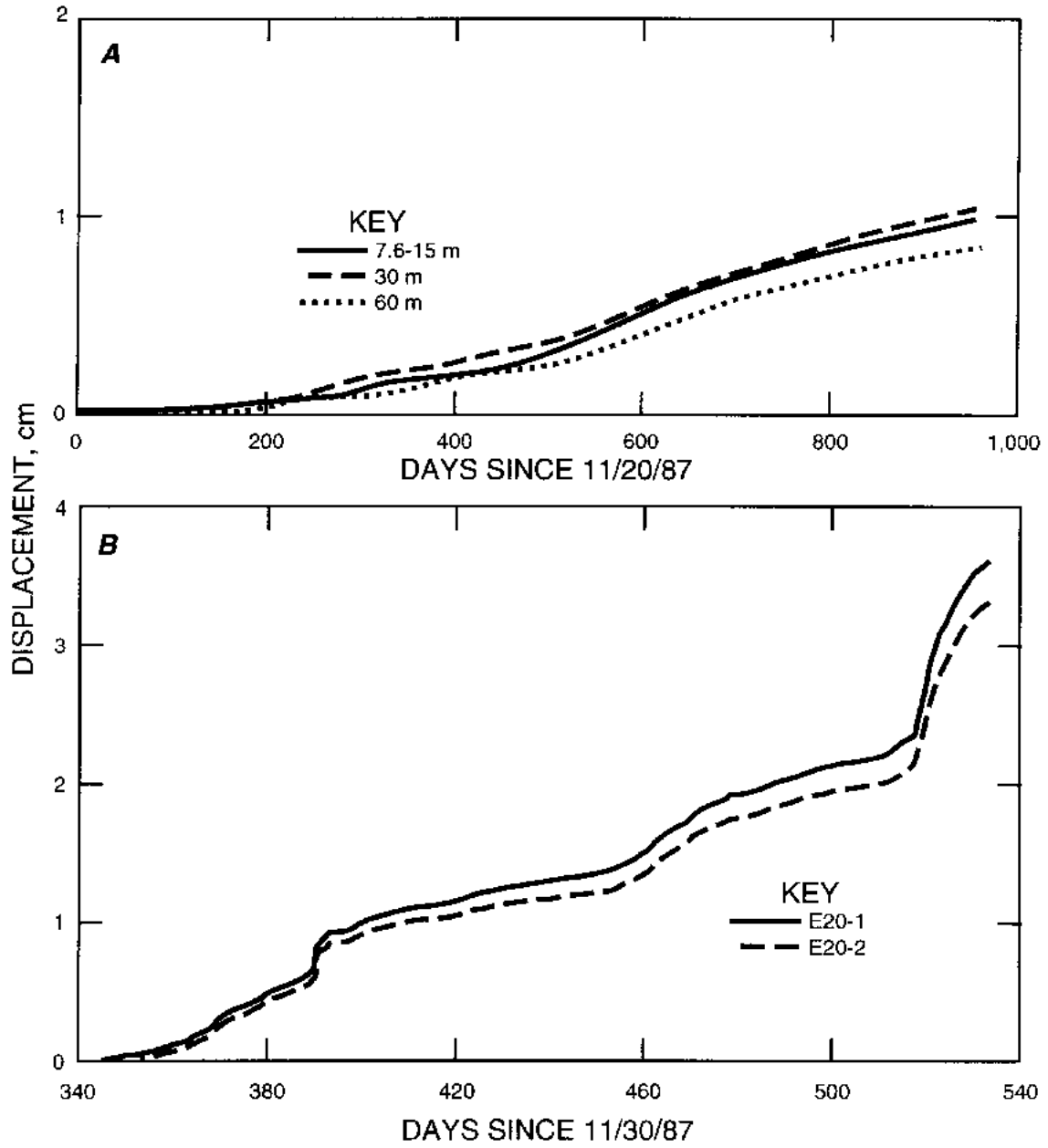*Comparison of coarse and insert meshes in calculations of shaft wall safety factors.*

Figure 7

Stresses on elements composing tunnel walls. A, Comparison of two- and three-dimensional stresses; B, location of centroid of elements surrounding tunnel.

Figure 8

Shaft extensometer layout.

Figure 9

Example extensometer data. A, Shaft extensometer (E1); B, stope extensometer (E20).

Figure 10
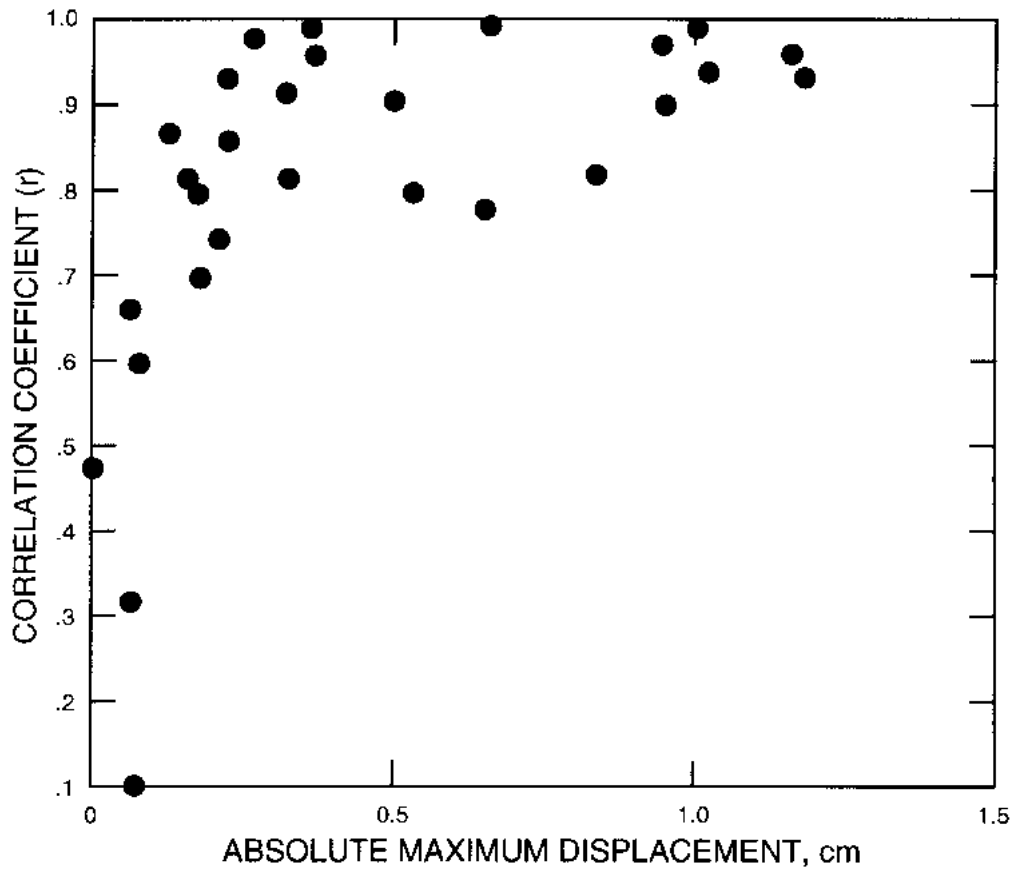
Correlation coefficient as function of extensometer anchor displacement.

Figure 11

A

60 m

Remote MPBX E1

30 m

15 m

Shaft

7.6 m

Shaft MPBX's

0   30

Scale, m

N

Ross shaft

PF

Sump

HF

30 m

HF

30 m

60-m stope
limit line

Previously
mined stopes

EF

HF

PF

North
wall

Central
pillar

18 m

South
wall

Motor
barn

Stope MPBX's

E20

LEGEND

EF   Ellison Formation

HF   Homestake Formation

PF   Poorman Formation

⬛   Ore-grade material

MPBX Multipoint
      borehole extensometer
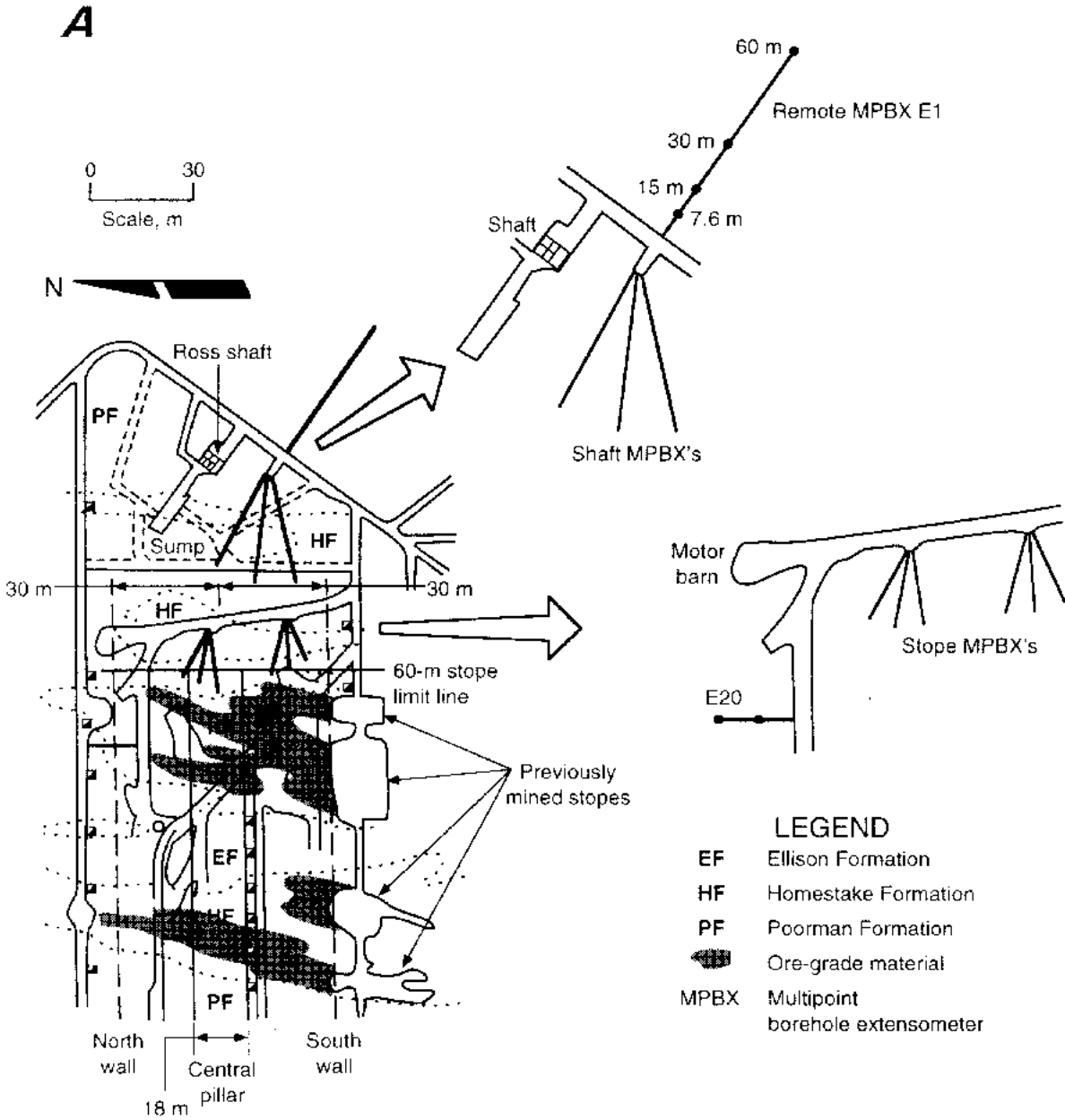
Ross shaft pillar. A, Plan view of 3650 level showing central pillar and placement of extensometers.

Figure 11—Continued

B
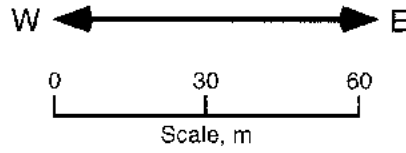
LEGEND

☐ Ellison Formation

▨ Homestake Formation

▨ Poorman Formation

■ Ore

▨ Wing pillar

W ⟷ E

0   30   60

Scale, m

3200 level

3350 level

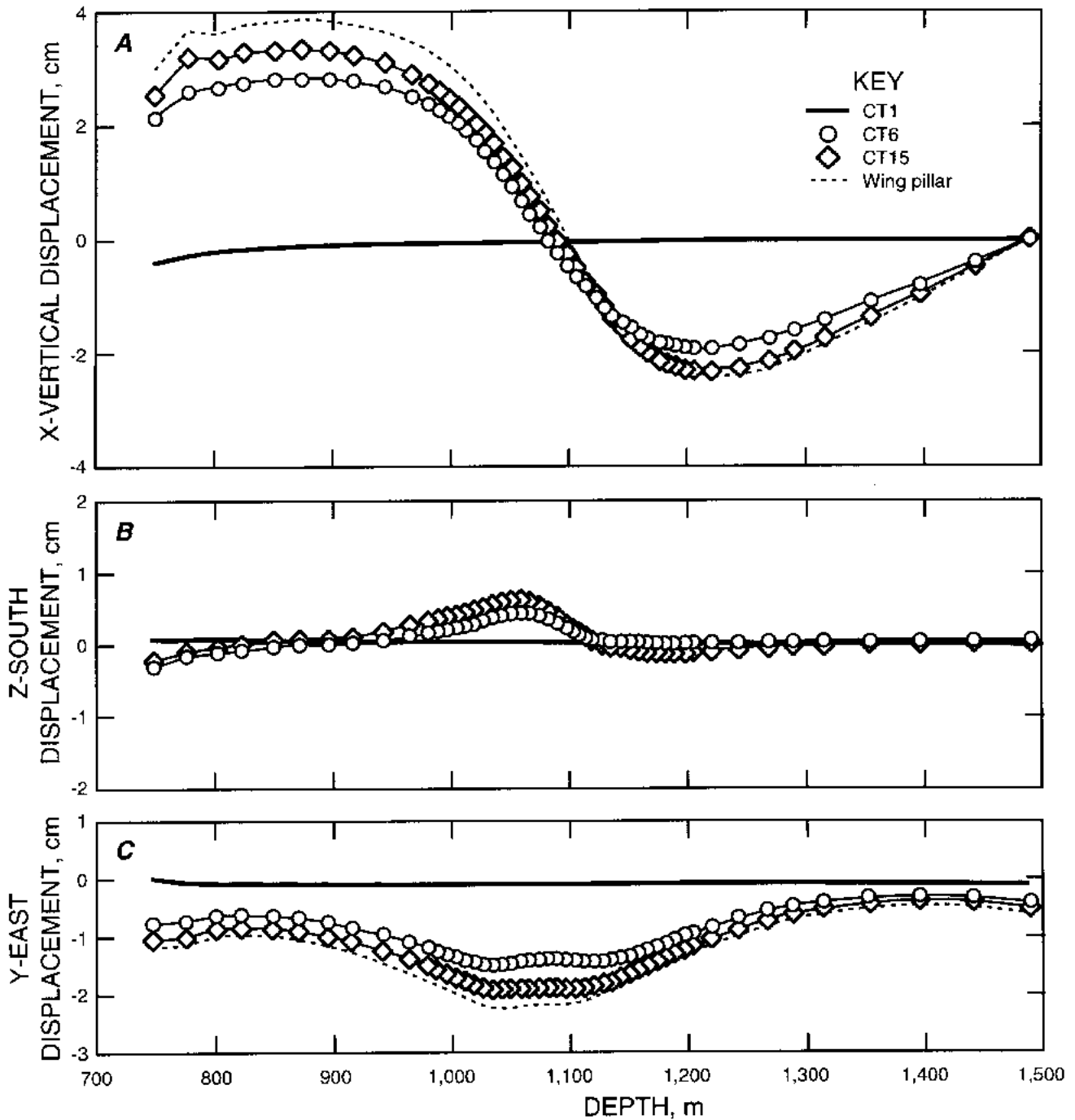3500 level

3650 level

3800 level

Ross shaft
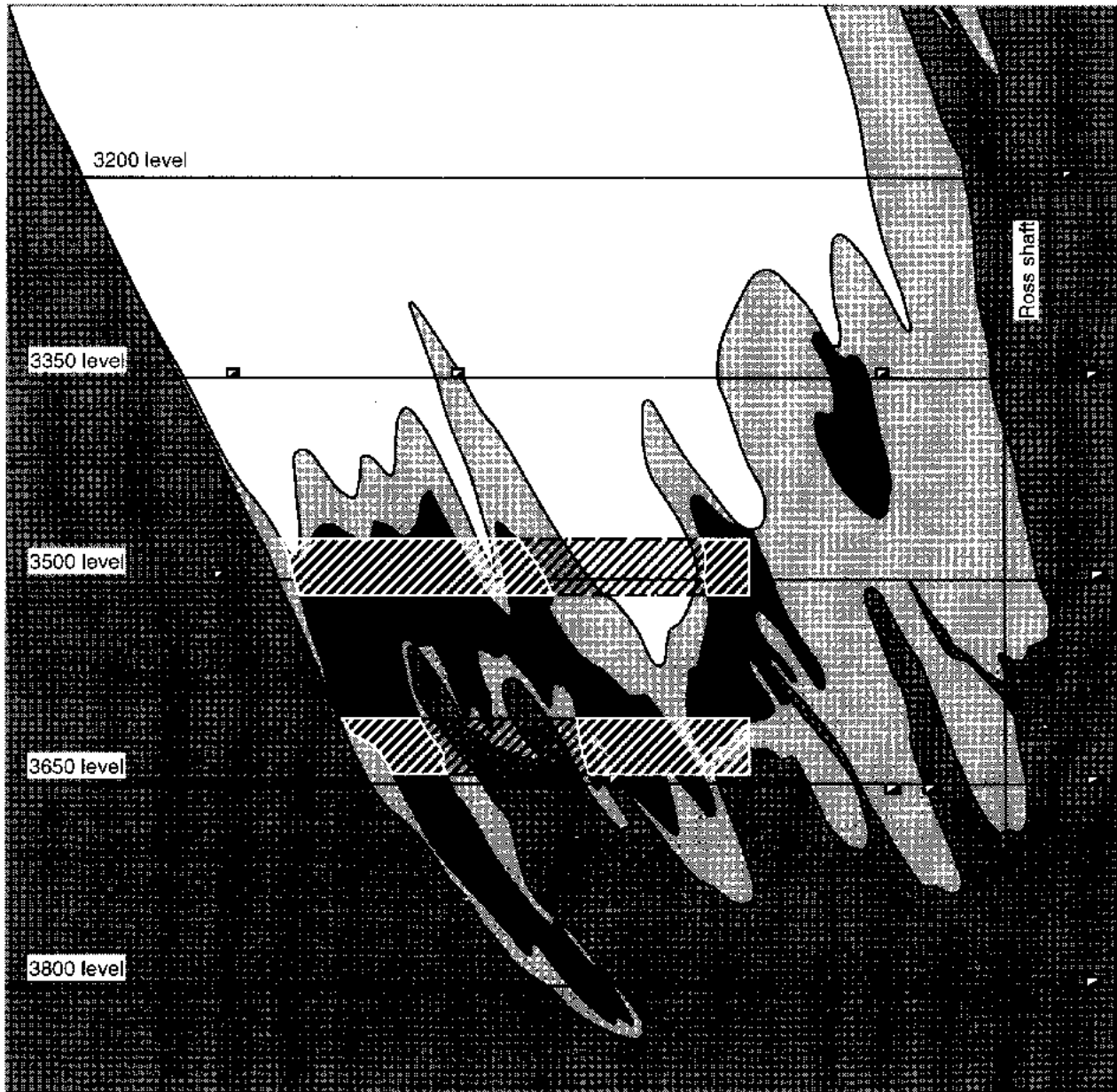
B, east-west vertical section showing wing pillars.

Figure 12
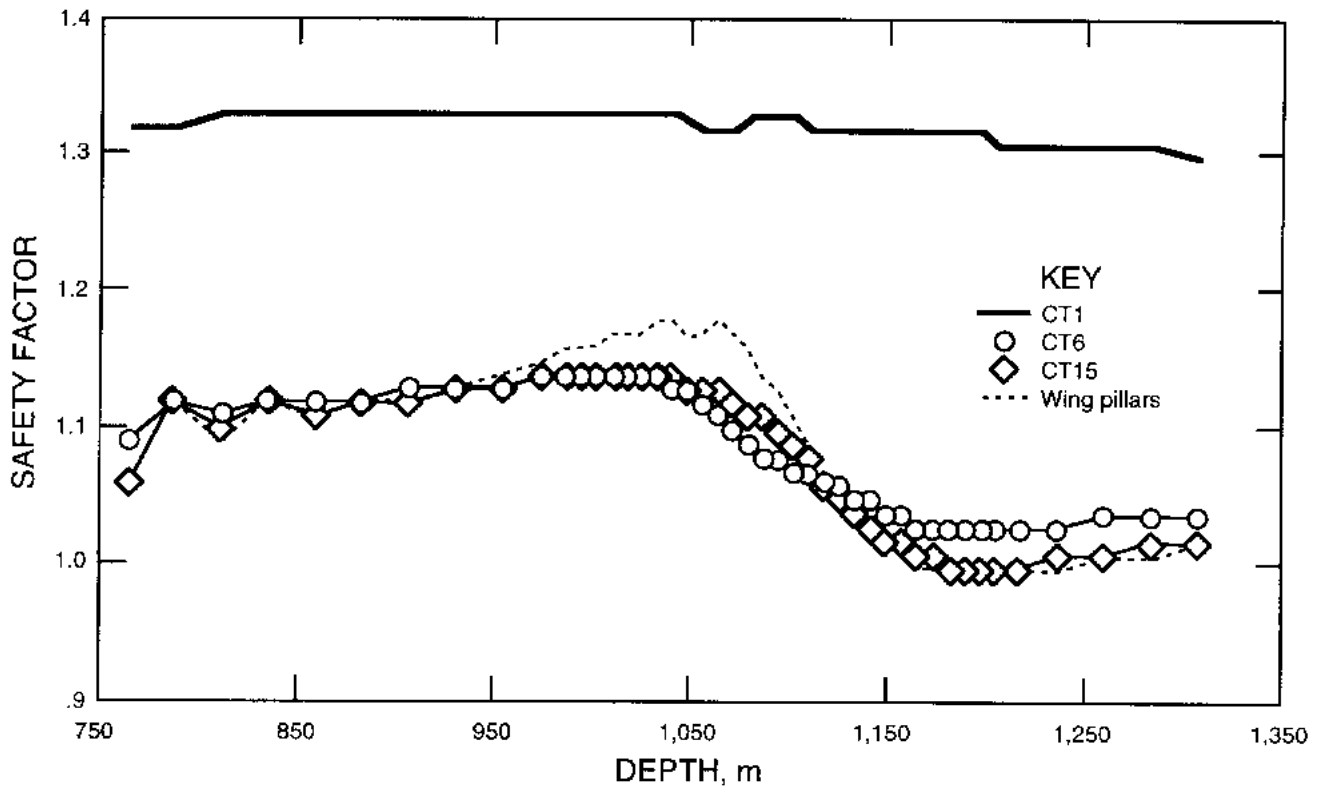
Shaft wall safety factor as function of depth. Lowest element (27) safety factor is plotted. Central and wing pillars left.

Figure 13

Shaft wall displacement, central pillar and two wing pillars left. A, Vertical; positive displacement indicates downward closure, negative is upward closure. B, North-south, parallel to strike; positive displacement indicates southern movement. C, East-west, perpendicular to strike; negative displacement indicates western movement toward pillar mining.
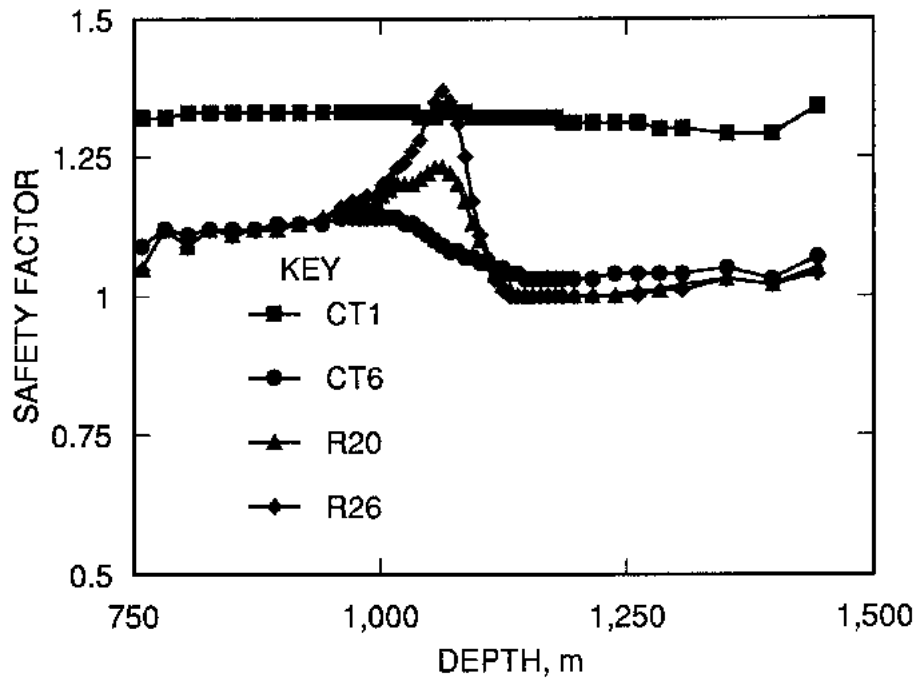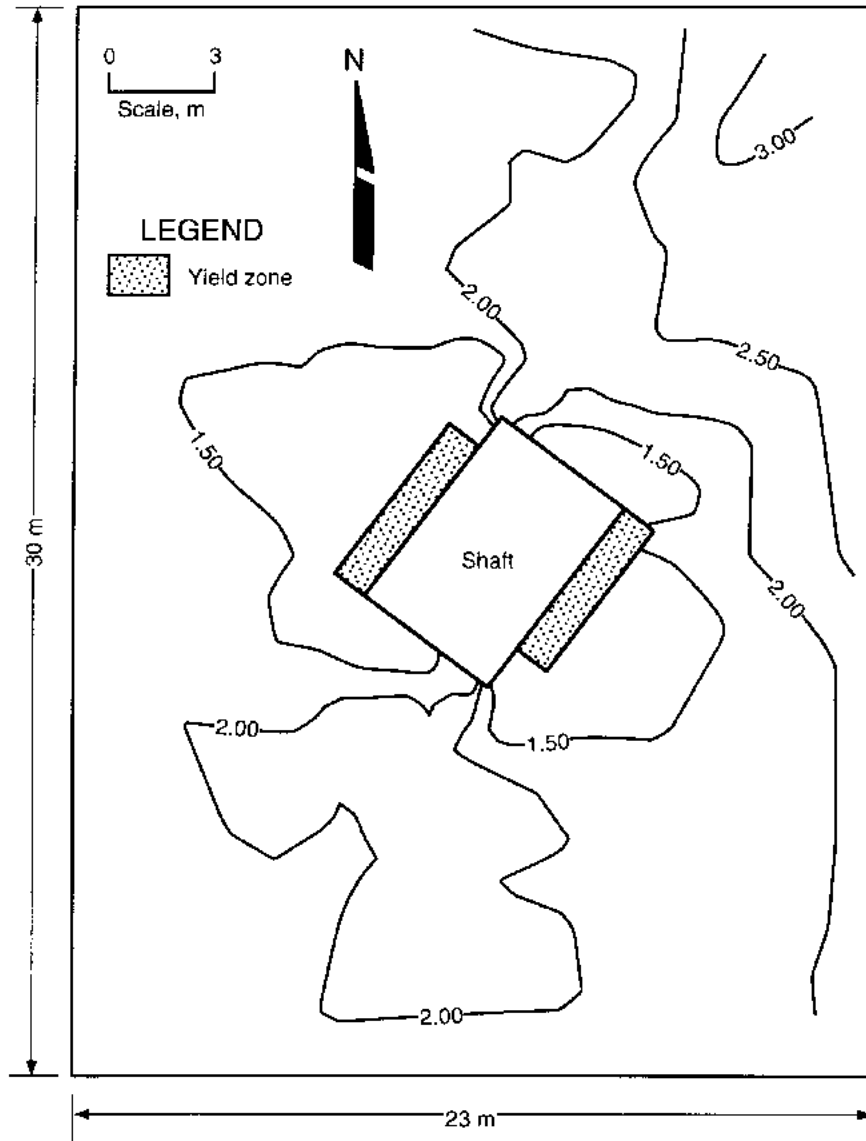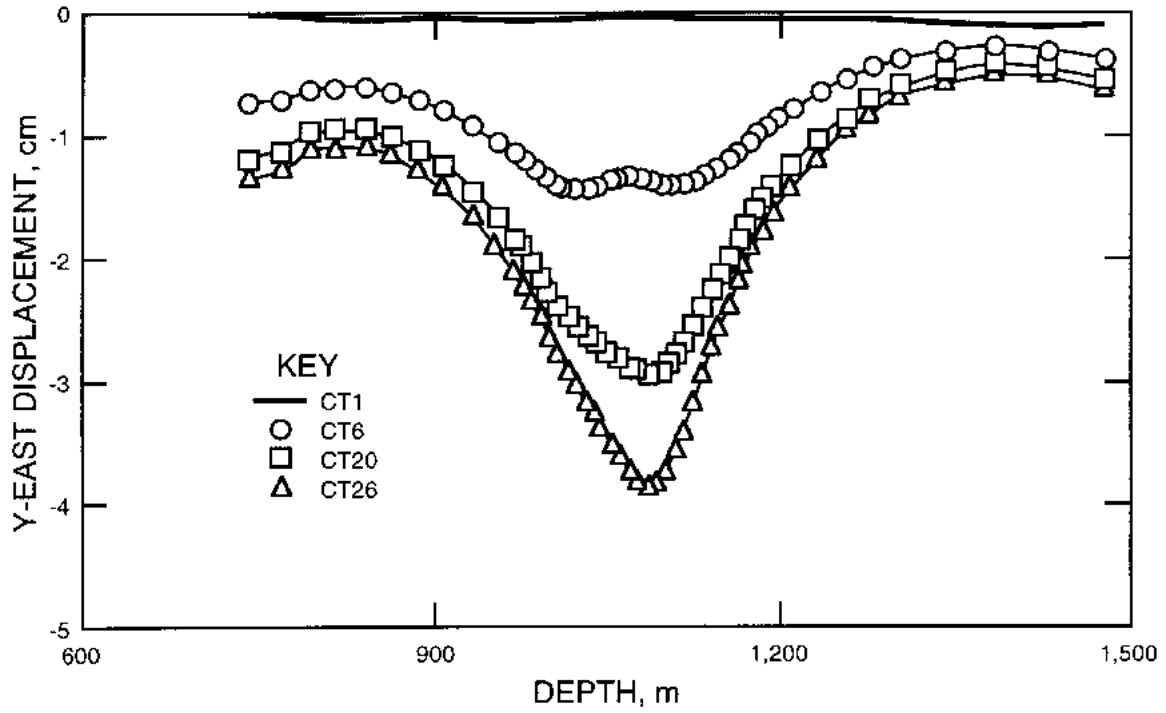
Figure 14

Shaft wall safety factor versus depth at various stages of mining.
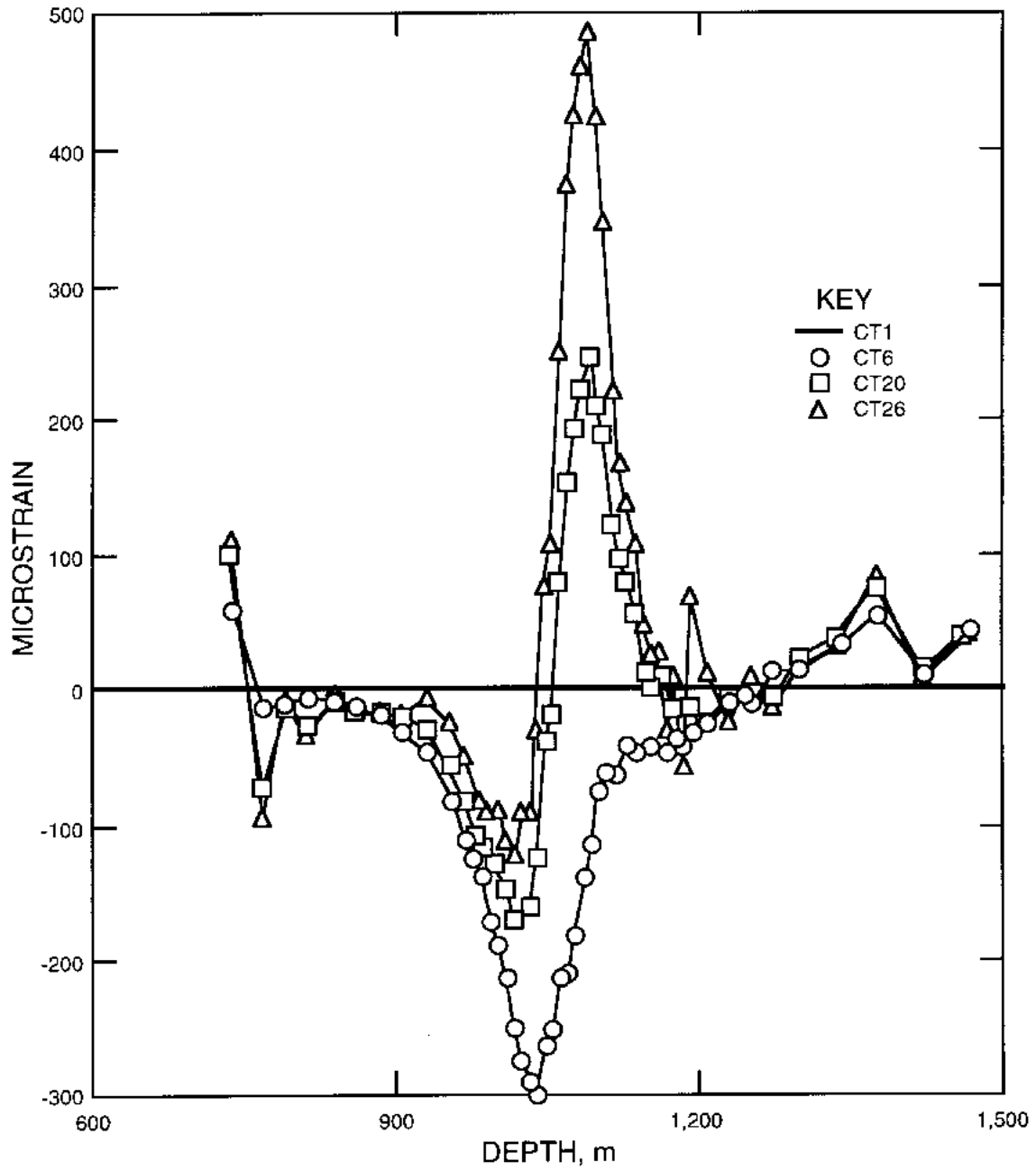
Figure 15

Calculated extent of yield zone after central pillar mining.

Figure 16

Shaft wall displacement versus depth at various stages of mining. Plus sign indicates movement to the east away from pillar mining; minus sign indicates movement to the west toward pillar mining.

Figure 17

Shaft strains versus depth at various stages of mining.